

# Solid Solutions Based on Bismuth and Antimony Chalcogenides above Room Temperature

L.N. Lukyanova, V.A. Kutasov, and P.P. Konstantinov  
*Ioffe Physical-Technical Institute, Russian Academy of Sciences,*  
*Polytekhnicheskaya 26, 194021 St.-Petersburg, Russia*  
 e-mail: [lidia.lukyanova@mail.ioffe.ru](mailto:lidia.lukyanova@mail.ioffe.ru)  
 Ph. +7 812 5159247, Fax +7 812 5156747

## Abstract

Thermoelectric properties of n -  $\text{Bi}_{2-x}\text{Sb}_x\text{Te}_{3-y-z}\text{Se}_y\text{S}_z$  and p-  $\text{Bi}_{2-x}\text{Sb}_x\text{Te}_3$  solid solutions are studied above room temperature. The increase in the figure-of-merit  $Z$  is shown to be observed in the compositions at the optimal relations between the average effective density-of-states-mass ( $m/m_0$ ), the mobility of carriers with account of degeneracy ( $\mu_0$ ), and the lattice thermal conductivity ( $\kappa_L$ ).

## Introduction

Solid solutions based on bismuth and antimony chalcogenides attract attention now since these materials are high-efficiency thermoelectrics at various substitutions of atoms in  $\text{Bi}_2\text{Te}_3$  sublattices at optimal compositions and charge carrier concentrations for operating both below and above room temperature. [1-3]. The dependence of  $Z$  behavior on carrier concentrations, temperature, and composition of solid solution [3-5] can be define from studies of the effective mass  $m/m_0$ , the carrier mobility  $\mu_0$ , and the lattice thermal conductivity ( $\kappa_L$ ), which are calculated with due to account of change of charge carrier scattering mechanism.

## 2. Thermoelectric properties in n-type solid solutions

Samples for studies were prepared by the directed crystallization method using precision stabilization of temperature at the front crystallization for growing of homogeneous ingots of solid solutions [6].

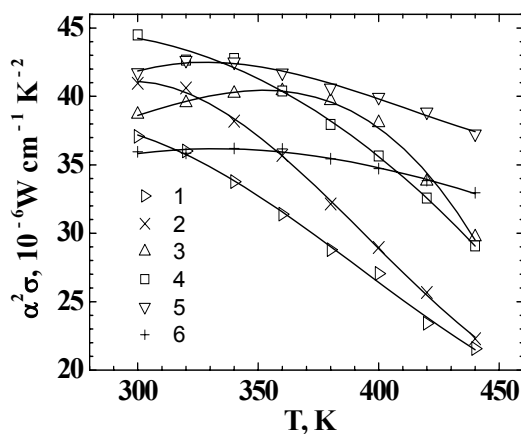


Figure 1. Temperature dependence of  $\alpha^2\sigma$ - factor in  $\text{Bi}_{2-x}\text{Sb}_x\text{Te}_{3-y-z}\text{Se}_y\text{S}_z$  solid solutions.

1 -  $x=0.16$ ,  $y=z=0.12$ , 2 -  $x=0.16$ ,  $y=z=0.06$ , 3 -  $x=y=0$ ,  $z=0.15$ , 4 -  $x=0$ ,  $y=z=0.09$ , 5-  $x=0$ ,  $y=z=0.15$ , 6 -  $x=0.2$ ,  $y=z=0.15$ .

$n$ ,  $10^{19} \text{ cm}^{-3}$ : 1 - 2.1, 2 - 2.2, 3 - 2.3, 4 - 4.9, 5 - 6.4, 6- 7.5.

An analysis of the Seebeck coefficient  $\alpha(T)$  and electrical conductivity  $\sigma(T)$  temperature dependences in the n - type solid solutions with atomic substitutions  $\text{Bi} \rightarrow \text{Sb}$  and  $\text{Te} \rightarrow \text{Se}$ ,  $\text{S}$  shows that power factor  $\alpha^2\sigma$  increases in the composition with less Se and S atoms (Figure 1, curves 5-6). The increase in the  $\alpha^2\sigma$ - factor in these samples is explained by more sharp temperature dependence of the electrical conductivity  $\sigma$  in comparison with compositions with more quantity of substituted atoms. A weak decrease in the  $\alpha^2\sigma$ - factor is observed in the samples with higher electron concentrations in comparison with lower concentrations (Figure 1, curves 5, 6 and 1-4).

Temperature dependences of the  $\alpha^2\sigma$ - factor (Figure 1) and thermal conductivity  $\kappa$  [3, 4, 7] define changes of  $Z$  values in multicomponent solid solutions.

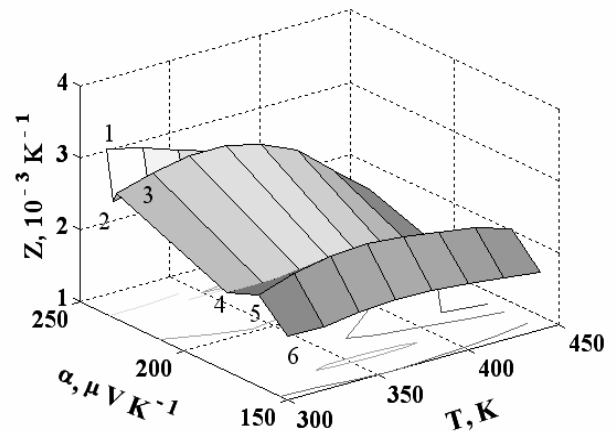


Figure 2. Temperature dependence of figure-of-merit  $Z$  in  $\text{Bi}_{2-x}\text{Sb}_x\text{Te}_{3-y-z}\text{Se}_y\text{S}_z$  solid solutions. Curve notation is the same as in Figure 1.

Study of thermal conductivity  $\kappa$  in dependence on composition and carrier concentration of  $\text{Bi}_{2-x}\text{Sb}_x\text{Te}_{3-y-z}\text{Se}_y\text{S}_z$  [3, 4, 7] shows that significant decrease in  $\kappa$  is observed in the compositions with substitutions of atoms in both sublattices with increase in quantity of the substituted atoms and with growth of carrier concentration. Therefore, despite of decrease in the power factor, low heat conductivity results in increase in the figure-of-merit for the composition at  $x=0.16$ ,  $y=z=0.12$  for temperatures up to 340 K (Figure 2, curve 1).

Value of  $Z$  grows in the composition with substitutions of atoms  $\text{Te} \rightarrow \text{Se}$ ,  $\text{S}$  at  $x=0$ ,  $y=z=0.15$  for temperature above 340 K at optimal electron concentration  $n$  (Figures 1, 2, curves 3). At further increase in temperature  $Z$  grows also for composition at  $x=0$ ,  $y=z=0.15$  in the sample with more

electron concentration (Figures 1, 2, curves 5). Reduction in the figure-of-merit at  $x=0$ ,  $y=z=0.09$  is explained with higher thermal conductivity owing to lower quantity of substituted atoms  $\text{Te} \rightarrow \text{Se}$ ,  $\text{S}$  despite of high power factor (Figure 1, 2, curves 4).

The increase in substituted Se and S atoms and growth of electron concentrations in solid solutions provide increasing in the figure-of-merit at high temperature, because the energy gap  $E_g$  grows for such compositions, and influence of the intrinsic conductivity occurs at higher temperatures [8].

### 3. Thermoelectric properties in the p-type solid solutions

Study of thermoelectric properties of p-  $\text{Bi}_{2-x}\text{Sb}_x\text{Te}_3$  solid solutions at low deviations  $x$  from 1.5 is shown to be observed the increase in the  $\alpha^2\sigma$ -factor with growth in hole concentrations and growth of substituted Sb atoms in the solid solutions (Figure 3, curves 5, 6).

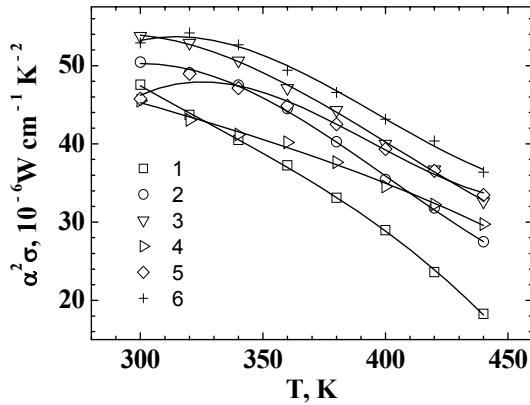


Figure 3. Temperature dependence of  $\alpha^2\sigma$ - factor in  $\text{Bi}_{2-x}\text{Sb}_x\text{Te}_3$ .  $x=1.5-1$ ,  $x>1.5-3-6$ .  $n$ ,  $10^{19} \text{ cm}^{-3}$ : 1 – 2.3, 2 – 3.6, 3 – 4.7, 4 – 6, 5 – 5.6, 6 – 6.3.

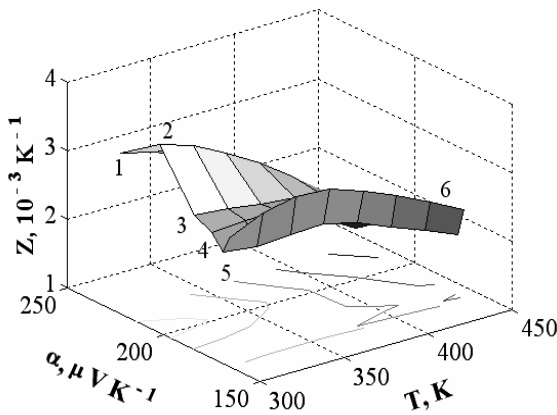


Figure 4. Temperature dependence of figure-of-merit  $Z$  in  $\text{Bi}_{2-x}\text{Sb}_x\text{Te}_3$  solid solutions. Curve notation is the same as in Figure 3.

Maxima on  $\alpha^2\sigma$  temperature dependences for high hole concentrations in the compositions at  $x>1.5$  specify by the beginning of the intrinsic conductivity at more high temperature in comparison with lower concentrations p (Figure 3, curves 5, 6 and 1-4).

Temperature dependence of the figure-of-merit  $Z$  in the p-type solid solutions is shown in Figure 4. Increase in  $Z$  near room temperature is observed in standard composition at  $x=1.5$  for optimal hole concentration (Figure 4, curve 2). At higher temperature  $Z$  value grows with increasing Sb content in the solid solutions ( $x>1.5$ ) and growth in hole concentrations (Figure 4, curves 5, 6).

### 4. Effective mass and carrier mobility in n-type solid solutions

The dependences of the average effective density-of-states-mass ( $m/m_0$ ), the carrier mobility with account of degeneracy ( $\mu_0$ ), and the lattice thermal conductivity ( $\kappa_L$ ) were calculated in terms of parabolic model of an energy spectrum with isotropic scattering of charge carriers [3-5]. These dependences were used for analysis of  $Z$  changes in the solid solutions.

In the calculations the effective scattering parameter ( $r_{\text{eff}}$ ) was used, which takes into account the changes of scattering processes in comparison with the acoustic scattering mechanism at substitutions of atoms in sublattices of  $\text{Bi}_2\text{Te}_3$ . The  $r_{\text{eff}}$  parameter was determined from the experimental data on galvanomagnetic effects together with the data on the Seebeck coefficient [9].

In the n-type solid solutions the effective mass  $m/m_0$  (Figure 5) increases with growth of electron concentration due to changing of anisotropy of the constant energy surface [10]. Weak decrease of  $m/m_0$  in dependence on temperature at high electron concentrations (Figure 5, curves 5, 6) in comparison with the samples with lower concentrations (Figure 5, curves 1-4) is explained by influence of the intrinsic conductivity with growth of temperature.

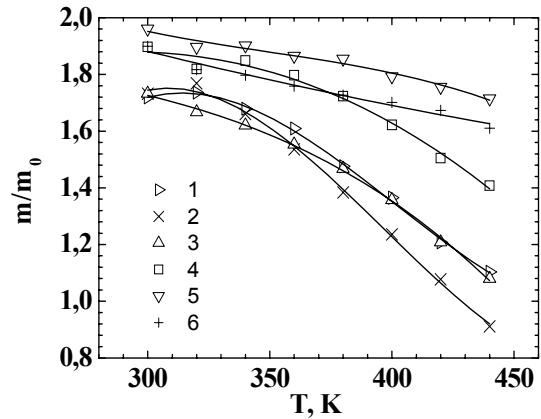


Figure 5. Temperature dependence of effective mass  $m/m_0$  in  $\text{Bi}_{2-x}\text{Sb}_x\text{Te}_{3-y-z}\text{Se}_y\text{S}_z$  solid solutions. Curve notation is the same as in Figure 1.

The carrier mobility  $\mu_0$  is decreased, and the dependence  $\mu_0(T)$  is weakened with growth of electron concentrations and with increase in quantity of the substituted atoms in the multicomponent solid solutions owing to additional scattering on neutral atoms of additional components and atoms alloying impurity (Figure 6).

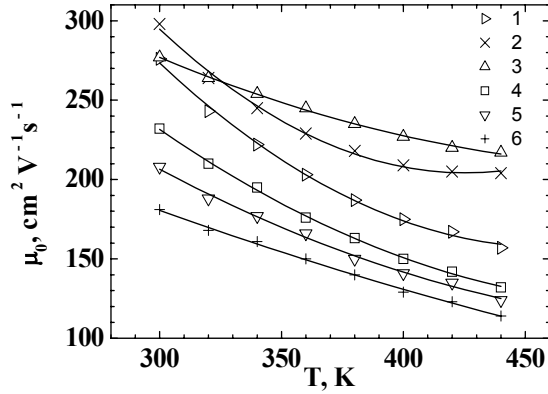


Figure 6. Temperature dependence of mobility  $\mu_0$  in  $\text{Bi}_{2-x}\text{Sb}_x\text{Te}_{3-y-z}\text{Se}_y\text{S}_z$  solid solutions. Curve notation is the same as in Figure 1.

### 5. Lattice thermal conductivity in n-type solid solutions

The distortions of the crystal lattice grow with increase in electron concentrations and quantity of atomic substitutions in solid solutions, and its result in increase of phonon scattering and decrease in the lattice thermal conductivity  $\kappa_L$  (Figure 7). Besides, the thermal conductivity ( $\kappa_{np}$ ) due to the intrinsic conductivity increases with temperature.

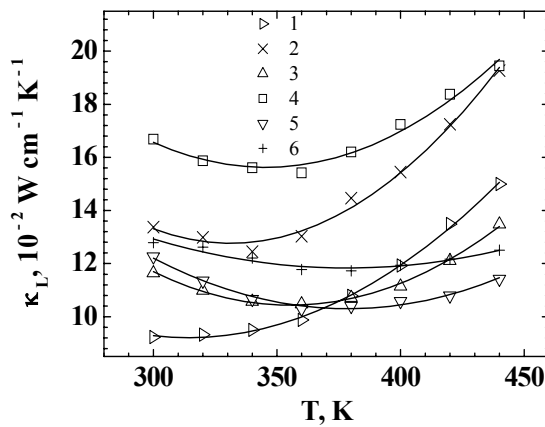


Figure 7. Temperature dependence of lattice thermal conductivity  $\kappa_L$  in  $\text{Bi}_{2-x}\text{Sb}_x\text{Te}_{3-y-z}\text{Se}_y\text{S}_z$  solid solutions. Curve notation is the same as in Figure 1.

Significant reduction of the  $\kappa_L$  value is observed in the compositions with atomic substitutions in both sublattices of  $\text{Bi}_2\text{Te}_3$  at  $x=0.16$ ,  $y=z=0.12$  in comparison with composition with smaller quantity of Se and S atoms (Figure 7, curves 1, 2). Growth of  $\kappa_L$  with increase in temperature ( $T > 370$  K) is explained by influence of the intrinsic conductivity in these samples at low electron concentrations.

At further increase in temperature low value of  $\kappa_L$  is observed for the composition ( $x=0$ ,  $y=z=0.15$ ) with higher electron concentration (Figure 7, curve 5). High lattice thermal conductivity in the composition at ( $x=0$ ,  $y=z=0.09$ )

is connected with smaller quantity of the substituted atoms and low electron concentrations (Figure 7, curve 4).

High  $\kappa_L$  value in the composition with increasing Sb content at ( $x=0.2$ ,  $y=z=0.15$ ) (Figure 7, curve 6) was observed as well as earlier in the compositions  $n\text{-Bi}_{2-x}\text{Sb}_x\text{Te}_3$  at  $x \geq 0.2$ .

In accordance with the obtained data on  $m/m_0$ ,  $\mu_0$  and  $\kappa_L$ , the value of  $Z$  grows in the composition ( $x=0.16$ ,  $y=z=0.12$ ) in the temperature range 300-370 K due to decrease of the lattice thermal conductivity  $\kappa_L$  and higher effective mass  $m/m_0$  in the sample with optimal electron concentration (Figures 4, 5, 7, curves 2).

Growth of the effective mass and low lattice thermal conductivity in the solid solution at  $x=0$ ,  $y=z=0.15$  with increase of electron concentration lead to increase of the figure-of-merit  $Z$  in the temperature range 370-450 K, despite of low carrier mobility (Figures 4, 5, 7, curves 4).

### 6. Effective mass and carrier mobility in p-type solid solutions

The effective mass  $m/m_0$  grows with increase of hole concentrations in the p-type solid solutions, as well as in  $n\text{-Bi}_{2-x}\text{Sb}_x\text{Te}_{3-y-z}\text{Se}_y\text{S}_z$  (Figure 8). The increase of  $x$  in p-type solid solutions also results in growth of  $m/m_0$ .

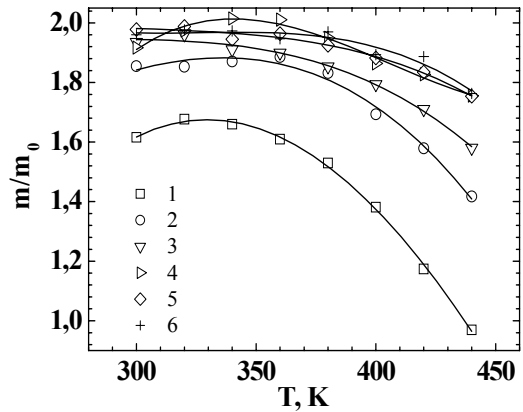


Figure 8. Temperature dependence of effective mass  $m/m_0$  in  $\text{Bi}_{2-x}\text{Sb}_x\text{Te}_3$  solid solutions. Curve notation is the same as in Figure 3.

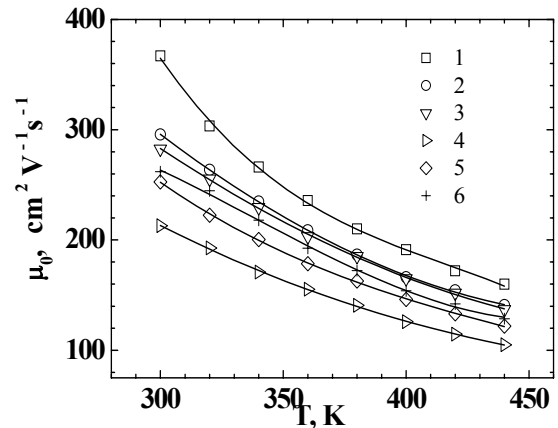


Figure 9. Temperature dependence of mobility  $\mu_0$  in  $\text{Bi}_{2-x}\text{Sb}_x\text{Te}_3$  solid solutions. Curve notation is the same as in Figure 3.

Weak temperature dependence  $m/m_0(T)$  in the compositions at  $x > 1.5$  with higher hole concentrations is explained by insignificant influence of the intrinsic conductivity in the considered temperature range (Figure 8).

The carrier mobility  $\mu_0$  is decreased and the dependence  $\mu_0(T)$  is weakened in the solid solutions  $\text{Bi}_{2-x}\text{Sb}_x\text{Te}_3$  with growth of hole concentration and Sb content (Figure 9).

### 7. Lattice thermal conductivity in p-type solid solutions

The lattice thermal conductivity  $\kappa_L$  in the  $\text{Bi}_{2-x}\text{Sb}_x\text{Te}_3$  solid solutions with low hole concentrations decreases at  $x = 1.5$  in comparison with the composition with more content of Sb atoms at  $T < 350$  (Figure 10, curves 1-3). Increase in hole concentrations together with growth in  $x$  in the solid solutions leads to decrease of  $\kappa_L$ -values (Figure 10, curves 4-6).

The relations between  $m/m_0$ ,  $\mu_0$  and  $\kappa_L$  values in the solid solutions  $\text{Bi}_{2-x}\text{Sb}_x\text{Te}_3$  at  $x = 1.5$  define the increase in  $Z$  near room temperature. The behavior of  $Z$  is explained by high carrier mobility  $\mu_0$  and its sharp temperature dependence  $\mu_0(T)$  at optimal hole concentration (Figure 4, 9, 10, curves 2).

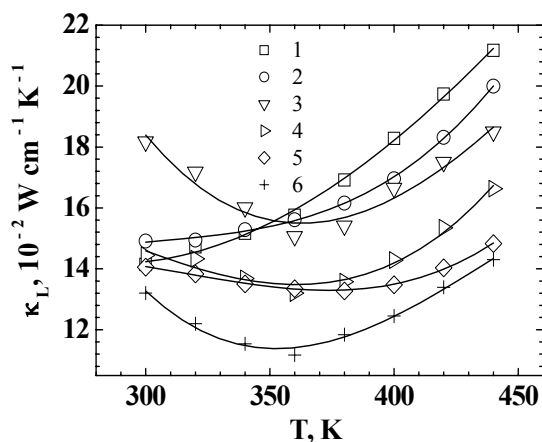


Figure 10. Temperature dependence of lattice thermal conductivity  $\kappa_L$  in  $\text{Bi}_{2-x}\text{Sb}_x\text{Te}_3$  solid solutions. Curve notation is the same as in Figure 3.

The value of  $Z$  grows in the solid solution with more atomic content of Sb atoms ( $x > 1.5$ ) and higher hole concentration for high temperatures due to growth of  $m/m_0$  and decrease in  $\kappa_L$  (Figure 4, 8, 10, curves 6).

### Conclusions

Thus, studies of n-  $\text{Bi}_{2-x}\text{Sb}_x\text{Te}_{3-y-z}\text{Se}_y\text{S}_z$  and p-  $\text{Bi}_{2-x}\text{Sb}_x\text{Te}_3$  solid solutions are shown to increase of the figure-of-merit  $Z$  in the compositions with the optimal relations between the average effective density-of-states-mass ( $m/m_0$ ), the mobility ( $\mu_0$ ), and the lattice thermal conductivity ( $\kappa_L$ ) at optimal charge carrier concentrations for operating interval of temperatures.

### Acknowledgments

This study was supported by Russian Foundation for Basic Research, projects No. 07-08-00191a.

### References

1. Ettenberg M.H., Jesser W.A., Rosi F.D. A New n-Type and Improved p-type Pseudo-ternary  $(\text{Bi}_2\text{Te}_3)(\text{Sb}_2\text{Te}_3)(\text{Sb}_2\text{Se}_3)$  Alloy for Peltier Cooling. *Proc. XV Int. Conf. on Thermoelectrics*, Pasadena, CA, USA, 52 (1996).
2. Svechnikova T.E., Shelimova L.E., Konstantinov P.P., Kretova M.A., Avilov E.S., Zemskov V.C., Shtive Kh., Zuber A., Müller E. "Thermoelectric Properties of Single Crystals for Solid Solutions  $(\text{Bi}_2\text{Te}_3)_{1-x-y}(\text{Sb}_2\text{Te}_3)_x(\text{Sb}_2\text{Se}_3)_y$ ". *Inorganic. Mater.*, Vol. 41, No. 10 (2005), pp. 1186-1193.
3. Kutasov V.A., Lukyanova L.N., Vedernikov M.V. "Shifting the Maximum Figure-of-Merit of  $(\text{Bi}, \text{Sb})_2(\text{Te}, \text{Se})_3$  Thermoelectrics to Lower Temperatures", Chapter 37, pp.37.1-37.18. In the *Thermoelectrics Handbook Macro to Nano*. Ed. by D.M. Rowe, CRC, Taylor & Francis Group, 2006.
4. Lukyanova L.N., Kutasov V.A., Konstantinov P.P. and Popov V.V. "Specific features in the behavior of the effective mass and mobility in n- $(\text{Bi}, \text{Sb})_2(\text{Te}, \text{Se}, \text{S})_3$ ". *Fiz. Tverd. Tela*, Vol. 48, No. 10 (2006), pp. 1751-1756. [*Phys. Solid State*, Vol. 48, No. 10 (2006), pp. 1856-1862].
5. Lukyanova L.N., Kutasov V.A., and Konstantinov P.P. "Effective Mass and Mobility of Carriers in p- $\text{Bi}_{2-x}\text{Sb}_x\text{Te}_{3-y}\text{Se}_y$  Solid Solutions at Temperatures below 300K". *Fiz. Tverd. Tela*, Vol. 47, No. 2 (2005), pp. 233-237. [*Phys. Solid State*, Vol. 47, No. 2 (2005), pp. 224-228].
6. Luzgin K.S., Kutasov V.A., Lukyanova L.N. "Precision Temperature Controller for Device of Vertical Zone Alignment". *Proc. of the VIII Interstate Seminar on Thermoelectrics and their Applications*, St. Petersburg, November (2002), pp. 275-280.
7. Lukyanova L.N., Kutasov V.A., and Konstantinov P.P. Effective Mass and Mobility in p- $\text{Bi}_{2-x}\text{Sb}_x\text{Te}_{3-y}\text{Se}_y$  Solid Solutions below Room Temperature. *Proceedings of the 8<sup>th</sup> European Workshop on Thermoelectrics*, Poland, Krakov, September 15-17, 2004, pp.147-149.
8. Becluder Ch.D., Goltsman B.M., Kutasov V.A., Petrov A.V., Energy Gap for Solid Solution  $\text{Bi}_2\text{Te}_{2.4}\text{Se}_{0.3}\text{S}_{0.3}$ . *Fiz. Tverd. Tela*, Vol. 16, No. 7 (1974), pp. 2121-2123.
9. Lukyanova L.N., Kutasov V.A., Popov V.V., and Konstantinov P.P. "Galvanomagnetic and Thermoelectric Properties of p- $\text{Bi}_{2-x}\text{Sb}_x\text{Te}_{3-y}\text{Se}_y$  Solid Solutions at Low Temperatures below ( $< 220\text{K}$ )". *Fiz. Tverd. Tela*, Vol. 46, No. 8 (2004), pp. 1366-1371. [*Phys. Solid State*, Vol. 46, No. 8 (2004), pp. 1404-1409].
10. Lukyanova L.N., Kutasov V.A., Popov V.V., and Konstantinov P.P. Galvanomagnetic and Thermoelectric Properties of Multicomponent n-type Solid Solutions Based on Bi and Sb Chalkogenides. *Tverd. Tela*, Vol. 48, No. 4 (2006), pp. 607-613. [*Phys. Solid State*, Vol. 48, No. 4 (2006), pp. 647-653].